Proceedings 10th NUMGE 2023
10th European Conference on Numerical Methods in Geotechnical Engineering
Zdravkovic L, Kontoe S, Taborda DMG, Tsiampousi A (eds)

https://doi.org/10.53243/NUMGE2023-143

Numerical modelling of drained and undrained cone penetration tests

X. Wu[1, 2], M. Ghafghazi[1], Z. Liu[1, 2], Y. Tian[2], S.H. Chow[2]

[1]*Department of Civil & Mineral Engineering, University of Toronto, Toronto, Canada*
[2]*Department of Infrastructure Engineering, The University of Melbourne, Melbourne, Australia*

ABSTRACT: The Cone Penetration Test (CPT) is a widely used in-situ test in geotechnical engineering because of its efficient application, continuous collection of multiple measurements, and repeatability. CPT results are affected by the soil drainage conditions around the cone. For intermediate particle size soils such as silts and tailings, interpretation of CPT results is challenging as partial drainage results in tip resistance and pore pressures in between fully drained and fully undrained conditions. Modelling the two extremes of drained and undrained cone penetration is the first key step of analysing whole drainage range of CPT. In this paper, drained and undrained CPT were simulated in Abaqus. The critical state based model, NorSand, was implemented as user subroutine VUMAT into Abaqus/Explicit. The Arbitrary Lagrangian Eulerian (ALE) scheme available in Abaqus/Explicit was utilized to prevent mesh distortions around the cone. The drained simulation results were validated against existing calibration chamber data on tailings. The pore water pressures in undrained conditions were computed and the effect of the drainage conditions on tip resistance and sleeve friction were discussed.

Keywords: CPT; drained and undrained conditions; finite element analysis; large deformation analysis; tailings

1 INTRODUCTION

The cone penetration test (CPT) is one of the most common in-situ methods in geotechnical engineering due to its efficient application, continuous collection of multiple measurements, and repeatability. The CPT measurements, tip resistance, sleeve friction and excess pore water pressure, can be interpreted to determine subsurface stratigraphy and estimate the engineering properties of soils. The interpretation of CPT results requires a comprehensive understanding of the cone penetration process. Finite element method (FEM) is a widely used approach to simulate the full penetration process while considering different contact, constitutive models, and drainage conditions. CPT in sands and clay has been simulated by FEM (e.g., Ahmadi and Golestani Dariani, 2017; Konkol and Bałachowski, 2017; Kouretzis et al., 2014; Liyanapathirana, 2009; Mozaffari and Ghafghazi, 2019) with various simplifying assumptions.

Among the available CPT modelling, simplified soil constitutive models have been used, e.g., Tresca and Modified Cam Clay for clay (Sheng et al., 2013), Mohr-Coulomb for sands (van den Berg, 1994). The use of advanced soil models has been limited (e.g., Fan et al., 2018) while it is necessary to reproduce realistic soil response. This is because during penetration, soil is undergoing density state change and mean and deviator stress change as well as principal stress rotation simultaneously.

NorSand is a critical state based constitutive model proposed by Jefferies (1993) and improved over the years (e.g., Jefferies and Shuttle, 2005). The state parameter, ψ, defined as the difference between the current void ratio and the void ratio at the critical state at the same confining stress, is central to NorSand. In this way, NorSand is capable of simulating the dilatancy of dense soils and contraction of loose soils. Therefore, cohesionless soils, such as unstructured and uncemented sands and silts, can be well simulated by NorSand. In this paper, NorSand was implemented in the user-defined subroutine for Abaqus/Explicit, VUMAT, and employed to simulate CPT penetration.

CPT measurements depend on the soil type and drainage conditions (Price et al., 2019; Sheng et al., 2014). Penetration in sands is normally assumed to be fully drained given their high permeability, while clay is considered as fully undrained condition due to its low permeability. The intermediate soils like silts, however, normally have a permeability between sands and clay, often result in partially drained CPT penetration conditions (DeJong and Randolph, 2012; Jaeger et al., 2010; Price et al., 2019). Before analysing the behaviour of CPT across the whole drainage condition, two extreme scenarios, the fully drained and the fully undrained conditions, should be analysed. In this paper, CPT in fully drained and undrained conditions were simulated in Abaqus/Explicit. In the fully undrained condition, the equivalent total stress method (Britto and Gunn, 1987) was employed.

Four cases including medium dense and loose under drained and undrained conditions were simulated. The tip resistances and sleeve frictions in fully drained conditions were validated against the chamber test results. The tip resistances and sleeve frictions in fully undrained conditions were predicted. The variation of the excess pore water pressure and its effect on the CPT results were discussed.

2 IMPLEMENTATION OF NORSAND IN VUMAT

NorSand has a bullet-shape of yield surface same as the original Cam Clay model (Shuttle and Cunning, 2007). Different from Cam Clay, the critical state line does not always intersect with the apex of the yield surface in NorSand. The yield surface of NorSand can move toward the critical state driven by a hardening law. The softening or hardening of the yield surface depends on the current state parameter and the loading direction (Shuttle and Cunning, 2007). This enables NorSand to capture the dilatancy of dense soils and the contraction of loose soils.

Mozaffari and Ghafghazi (2017) implemented NorSand into the user-defined subroutine for Abaqus/Explicit, VUMAT. The cutting plane return mapping algorithm (CPA) proposed by Simo and Taylor (1986) was employed in VUMAT. In this paper, the NorSand VUMAT was programmed in a similar way. The version of NorSand used in the present work corresponds to the updated version in Jefferies and Been (2015). Due to the absence of pore water pressure as a degree of freedom and hence lacking coupled hydromechanical analysis, soils in partially drained and undrained conditions cannot be directly simulated in Abaqus/Explicit. In order to simulate soil behaviour in fully undrained condition in a simple way, pore water pressure was introduced as a variable in the subroutine, and the equivalent total stress method (Britto and Gunn, 1987) was employed in VUMAT. The flowchart of this method is given in Figure 1. At the beginning of VUMAT, pore water pressure is subtracted from total stress to calculate effective stress. The calculated effective stress is transferred into CPA to update the stress state. After that, pore water pressure increment is calculated by the product of volumetric strain increment and bulk modulus of water. The total stress is updated by adding the new pore water pressure to the new effective stress and returned back to Abaqus. In this way, the total volumetric strain is transferred to pore water pressure and the undrained behaviour of soil is simulated.

The drained and undrained triaxial compression tests were simulated to verify the developed VUMAT. Jefferies and Been (2015) provided a Visual Basic code (VBA) with NorSand implemented. For both drained and undrained tests, one loose soil and dense soil were simulated in Abaqus/Explicit and compared with VBA results. The input parameters are summarized in Table 1. Figure 2 shows the comparison of the results from Abaqus and VBA. The good agreement is seen as the validation of the developed VUMAT and the confirmation of the equivalent total stress method.

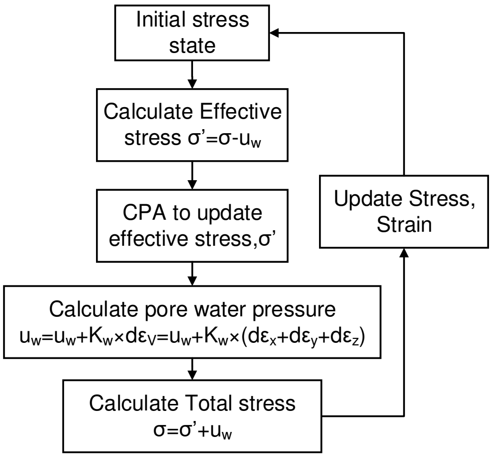

Figure 1. The flow chart of the equivalent total stress method.

Table 1. Input parameters for verification.

	Dense	Loose
ψ	-0.2	0.07
Γ	0.855	
λ	0.021	
M_{tc}	1.27	
N	0.4	
χ_{tc}	4	
H_0	120	
H_ψ	0	
G_{ref} (MPa)	60	
G_{exp}	0.4	
ν	0.2	

3 MODELLING OF CPT PENETRATION

The numerical model replicated Ayala et al. (2020)'s work who modified a triaxial testing machine to conduct a series of miniature CPT tests in tailings. The tailings sample had a 0.2 m diameter and 0.3 m height. The cone's diameter, d_c, was 0.01 m. A 100 kPa effective pressure was applied to the soil to consolidate different void ratios. After consolidation, the cone penetrated into the tailings at a 0.0002 m/s rate.

3.1 Geometry, loading and boundary conditions

The model is axisymmetric, and the cone started above the soil surface. The boundary conditions are shown in Figure 3. The vertical displacement of the soil bottom surface was restricted. The right surface of the soil had a constant pressure (100 kPa) boundary condition, mimicking the boundary condition in the miniature CPT tests. The 100 kPa consolidation surcharge was applied on the top surface of the soil. The vertical and horizontal components of the geostatic stress were 100 kPa and K_0 was 1.0. The initial pore water pressure within the soil was assumed as 0 kPa. The cone was allowed to move in the vertical direction and the horizontal direction displacement was constrained. A displacement rate of 0.001 m/s was applied to the cone top surface and cone penetrated for 0.13 m ($13d_c$), which is greater than Ayala et al (2020). This did not affect the CPT results but can reduce the simulation time.

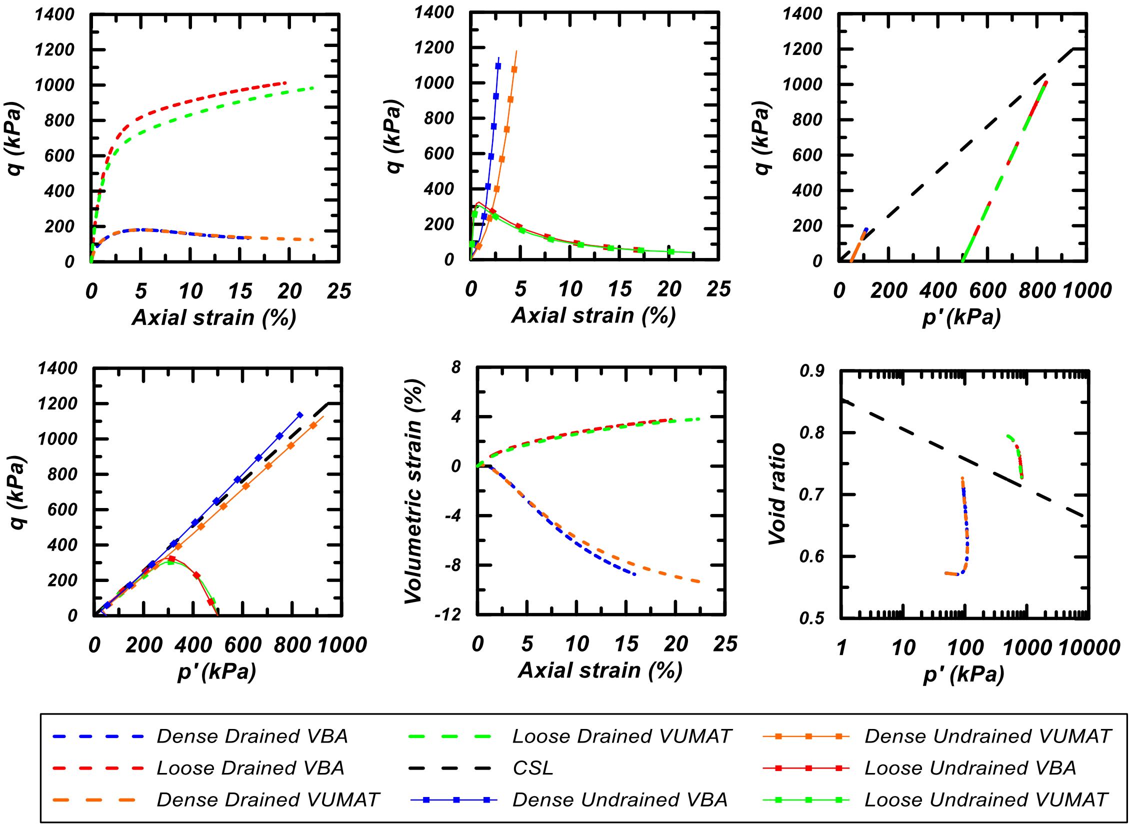

Figure 2. Comparison of TC test results from VUMAT and VBA.

Potyondy (1961) conducted shear tests on silt-steel interfaces and their results showed the friction angle for the silt-smooth steel interface is about 20°. Therefore, the friction coefficient, μ, was adopted as 0.37 (i.e., $\mu = \tan 20^{\circ}$) for the soil-cone contact in this model.

3.2 ALE and Mesh setup

The large deformation of soil makes CPT penetration difficult to simulate because it can result in excessive mesh distortion in simulation. The Arbitrary Lagrangian Eulerian method (ALE) available in Abaqus (Dassault Systèmes Simulia Corp., 2021) was employed to solve the large deformation and mesh distortion problem. In this model, a small gap with a 0.001 mm width was left between the soil and the symmetry axis because otherwise the element next to the symmetry axis will be distorted as ALE does not change the topology of the mesh. In other words, the soil and cone were 0.001 mm away from the symmetry axis. A rigid wall was set up on the left surface of the soil to prevent the leftward displacement of the soil. This way the nodes on the left surface of the soil can closely satisfy the axisymmetric condition and move in the horizontal direction freely in ALE to solve the mesh distortion.

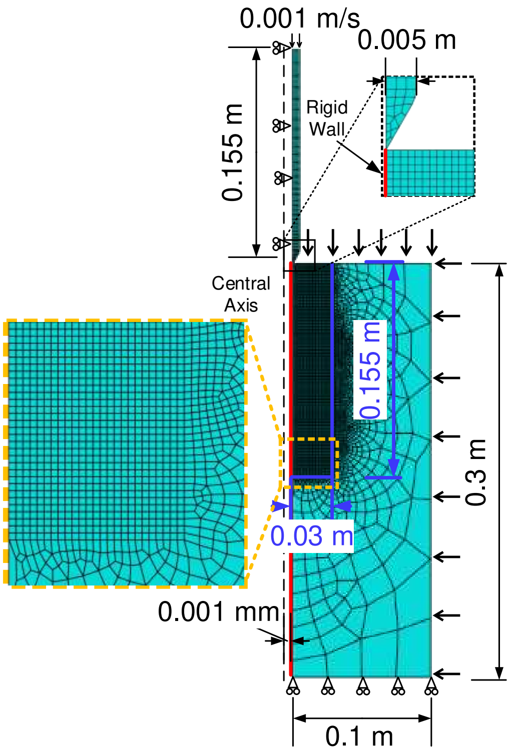

Figure 3. The model geometry and boundary conditions in simulation.

ALE was applied to the adaptive region which was 0.03 m in width and 0.155 m in height as shown in Figure 3. In this region, a finer mesh was used to get a precise result. The length of mesh was set as 0.0012 m and uniform mesh was applied to this region. In other regions, a coarser mesh was employed to optimize simulation time. A 4 nodes axisymmetric quadrilateral element (CAX4R) was applied to both regions. The parallelization simulation with 16 processors was employed to speed up the modelling. Each case took 4 to 6 hours to finish.

4 VALIDATION BASED ON DRAINED PENETRATION

4.1 Input parameters

Undrained or partially drained calibration chamber data are rare and unavailable with reliable accompanying data that are needed for calibrating constitutive models. Hence the validation was done on drained penetration data from the gold tailings from an operational mine in Australia used as the testing material in Ayala et al. (2020). The tailings material is a low-plasticity sandy silt. The soil properties were summarized in Table 2.

Table 2. General properties of the gold tailings.

Property	Gold tailings
Specific gravity	2.78
Liquid limit (%)	18
Plastic limit (%)	16
Plastic index (%)	2
Percent<75 (μm)	58
Percent<38 (μm)	44
D_{50} (μm)	50

Two cases, one medium dense case and one loose case, were simulated to validate the VUMAT. The state parameter for the medium dense case was -0.049 and for the loose case was 0.019. Ayala et al. (2022) calibrated NorSand to these tailings as summarized in Table 3. In NorSand, the shear modulus, G, is an important parameter to describe the elastic behaviour of soil. Equation (1) was employed to account for the influence of confining pressure on the shear modulus. G_{ref} is the reference shear modulus when effective pressure, p', is equal to 100 kPa. G_{exp} is the shear modulus exponent. The input parameters for medium dense and loose cases are summarized in Table 3. Ayala et al. (2022) reduced G_{ref} by a factor of four for obtaining better results following the advice of Shuttle and Jefferies (2016). In our analyses, a tenfold reduction was applied, consistent with Mozaffari and Ghafghazi (2023).

$$G = G_{\text{ref}} \cdot \left(\frac{p'}{100\text{kPa}}\right)^{G_{\text{exp}}} \tag{1}$$

The cone itself was simulated using the linear elastic model. The elastic modulus of steel is 180 GPa, and Poisson's ratio was set as 0.3. The elastic modulus was input as 18 GPa in the simulations. The reduction can increase the critical time increment required for stable calculations in the explicit scheme, so that it can improve the stability. The simulation results are not affected by the reduction in the cone elastic modulus.

Table 3. Input parameters used in the simulation.

	Medium dense	Loose
ψ	-0.049	0.063
e	0.572	0.684
Γ	0.796	
λ	0.038	
M_{tc}	1.45	
N	0.21	
χ_{tc}	5	
H_0	60	
H_ψ	420	
G_{ref} (MPa)	41	
G_{exp}	0.68	
ν	0.2	

4.2 Interpretation of the results

The tip resistance, q_c, and the sleeve friction, f_s, from simulations were compared with that from mini-chamber data described earlier in Figure 4. The tailings were deposited in three separate layers in Ayala et al. (2020) and the cone penetration occurred in the middle layer to avoid the effect of the top and bottom rigid boundary conditions. Therefore, only the tip resistances in steady state were reported by Ayala et al. (2020). The tip resistance for the medium dense tailings from modelling was 6 MPa, which is very close to the measured value, 5.4 MPa. For the loose tailings, the simulated tip resistance is around 3 MPa, which is close to the measured value, 2.7 MPa. The difference may result from the boundary conditions. A rigid top cap was on the top surface of soils in the mini chamber tests and a pressure (i.e., 100 kPa) was applied on it as in a typical triaxial tests. In the simulation, a stress boundray condition (i.e., 100 kPa surcharge) was applied on the top surface in simulation. The rigid top cap may affect the tip resistances. Only the sleeve friction of the loose tailings was reported by Ayala (2022). The simulated sleeve friction is 40 kPa, which is higher than the measured value, 27 kPa. The reason is that the used friction coefficient may be higher than that in real condition.

5 THE FULLY UNDRAINED CPT SIMULATION

The fully undrained CPT was modelled by using the equivalent total stress method. The boundary conditions were identical to the fully drained CPT simulation. Similar to the miniature chamber tests conducted for the fully drained CPT, the fully undrained cone penetration was assumed to also undergo a consolidation stage. Therefore, the initial pore water pressure, u_0, was uniformly set to 0 kPa for both the fully drained and undrained CPT simulations.

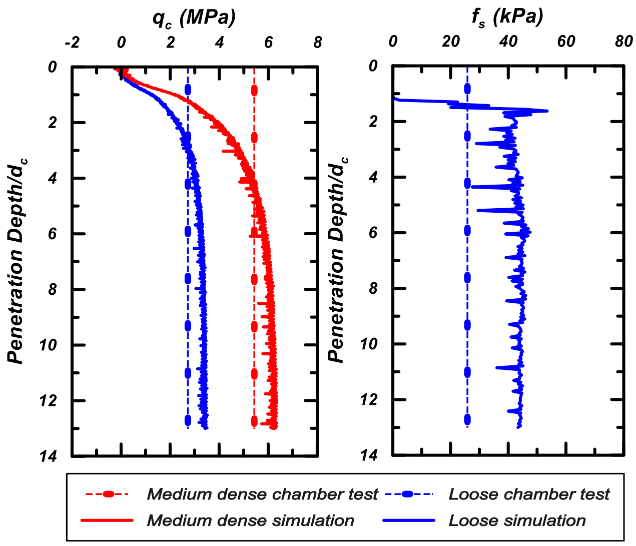

Figure 4. The comparison of the normalized tip resistance from measurement and simulation.

The tip resistance, q_c, and sleeve friction, f_s, under undrained conditions were compared to the drained values in Figure 5. The tip resistances of both the medium dense tailings and loose tailings in the fully undrained are lower than that in the fully drained condition. For the loose tailings, positive pore water pressure was detected below and behind the cone. For the medium dense tailings, a positive pore water pressure was observed below the cone tip, but a negative pore water pressure (u_2) was detected behind the cone, as expected (Figure 6). The positive excess pore pressure ahead of the cone may explain the reduction in tip resistance in both cases.

The undrained tip resistance for the medium dense tailings was about 0.3 times that of the drained tip resistance. For the loose tailings, the ratio between the tip resistance in undrained condition and drained condition was about 0.12. Dienstmann et al. (2018) compiled CPT results in contractive gold tailings under different drainage conditions. They reported the ratio between the tip resistance in undrained and drained conditions to be between 0.1 and 0.18, which is close to the simulation results for the loose tailings.

For the loose tailings, u_2 is 250 kPa. For the medium dense tailings, u_2 is -200 kPa. The excess pore water pressure, Δu_w, was normalized as pore water pressure coefficient, B_q, by Equation (2). B_q for loose tailings and medium dense tailings are 0.8 and -0.1, respectively. Based on these values, the type of soil can be estimated as contractive soil and moderately dilative soil for loose and medium dense tailings.

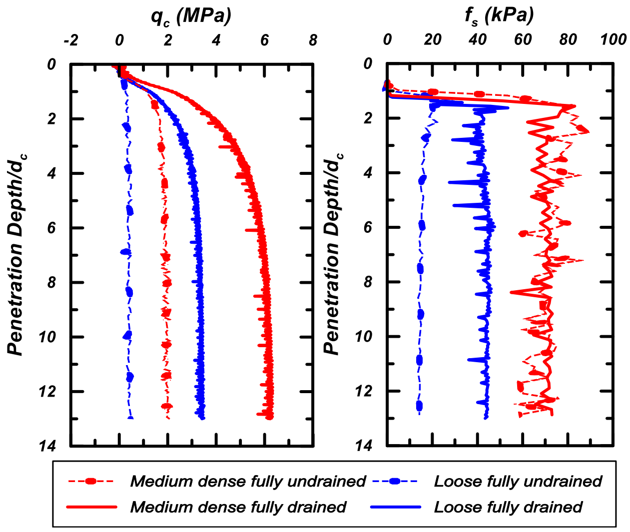

Figure 5. The comparison of CPT measurements for medium dense tailings ($\psi = -0.049$) and loose tailings ($\psi = 0.019$) under fully drained and fully undrained conditions.

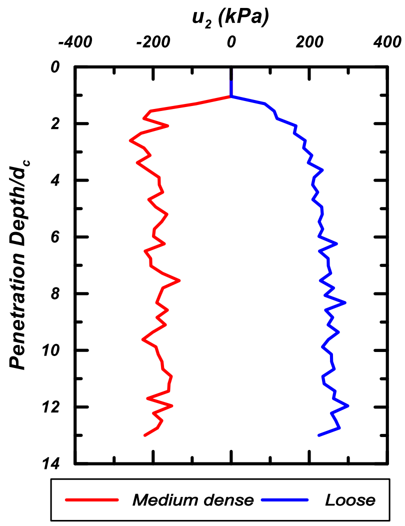

Figure 6. The pore water pressure, u_2, from CPT for medium dense tailings ($\psi = -0.049$) and loose tailings ($\psi = 0.019$).

$$B_q = \frac{\Delta u_w}{q_c - \sigma_{v0}} = \frac{u_2 - u_0}{q_c - \sigma_{v0}} = \frac{u_2}{q_c - \sigma_{v0}} \quad (2)$$

where σ_{v0} is the total vertical stress.

There is a limitation in the fully undrained CPT simulations. As mentioned above, the total stress was returned to Abaqus after the equivalent total stress method. Therefore, the total stress, not the effective stress, was used to calculate the friction at the interface, which means the sleeve frictions computed are not realistic in undrained analyses.

6 CONCLUSIONS

NorSand, a critical state based model for cohesionless soil, was programmed into the user-defined subroutine for Abaqus/Explicit, VUMAT. The pore water pressure was introduced into VUMAT and the equivalent total stress method was used to simulate the soil behaviour in fully undrained condition. The implementation was verified for loose and dense, and drained and undrained triaxial tests and used to model cone penetration test.

The developed VUMAT was numerically stable to model CPT penetration where other numerical difficulties, including soil-cone contact, and mesh distortions were appropriately solved. The simulated tip resistances and sleeve friction during drained penetration were compared with mini-chamber data on a tailings. The tip resistance showed good agreement while the sleeve friction was slightly higher than the measured value.

The equivalent total stress method was used to predict CPT measurements in the fully undrained condition. The simulated results showed that the tip resistance of loose and medium dense tailings in the fully undrained condition is lower than that in the fully drained condition.

Future work will include implementing NorSand in Abaqus/Standard, so that the coupled hydromechanical analysis can be employed to capture the undrained and partially drained penetration more realistically.

7 ACKNOWLEDGEMENTS

Authors express their sincere gratitude to ConeTec, WSP, and Vale and Office of the VP International (OVPI) at University of Toronto for Toronto-Melbourne joint training program for enabling this research.

8 REFERENCES

Ahmadi, M.M., and Golestani Dariani, A.A. 2017. Cone penetration test in sand: A numerical-analytical approach. *Computers and Geotechnics* **90**, 176–189.

Ayala, J. 2022. *Assessment of the state parameter in mine tailings using cone penetration tests with calibration chambers*. The University of Western Australia, Perth, Australia

Ayala, J., Fourie, A., and Reid, D. 2020. Cone penetration testing on silty tailings using a new small calibration chamber. *Géotechnique Letters* **10**, 492–497.

Ayala, J., Fourie, A., and Reid, D. 2022. Improved cone penetration test predictions of the state parameter of loose mine tailings. *Canadian Geotechnical Journal* **59**, 1969–1980.

van den Berg, P. 1994. *Analysis of soil penetration*. Delft University of Technology, Delft, Netherlands

Britto, A. M., and M. J. Gunn. 1987. *Critical state soil mechanics via finite elements*. Chichester, West Sussex, UK.

Dassault Systèmes Simulia Corp. 2021. *Abaqus User's Manual*. Providence, Rhode Island, USA.

DeJong, J.T. and Randolph, M., 2012. Influence of partial consolidation during cone penetration on estimated soil behavior type and pore pressure dissipation measurements. *Journal of Geotechnical and Geoenvironmental Engineering*, **138**, 777-788.

Dienstmann, G., Schnaid, F., Maghous, S., and Dejong, J. 2018. Piezocone Penetration Rate Effects in Transient Gold Tailings. *Journal of Geotechnical and Geoenvironmental Engineering*, **144**, 04017116.

Fan, S., Bienen, B. and Randolph, M.F., 2018. Stability and efficiency studies in the numerical simulation of cone penetration in sand. *Géotechnique Letters*, **8**, 13-18.

Jaeger, R., Dejong, J., Boulanger, R., Low, H.E., and Randolph, M. 2010. Variable penetration rate CPT in an intermediate soil. *Proceedings, 2nd International Symposium of the Cone Penetration Test* (Eds: Robertson P.K. & Mayne P.W.), 2-50. Huntington Beach, CA, USA.

Jefferies, M., and Been, K. 2015. *Soil Liquefaction: A Critical State Approach, Second Edition*. CRC Press, London.

Jefferies, M., and Shuttle, D. 2005. NorSand: Features, Calibration and Use. *Soil Constitutive Models: Evaluation, Selection, and Calibration*. 204–236.

Jefferies, M.G. 1993. Nor-Sand: a simple critical state model for sand. *Géotechnique* **43**, 91–103.

Konkol, J., and Bałachowski, L. 2017. Numerical Modeling of Cone Penetration Test in Slightly Overconsolidated Clay with Arbitrary Lagrangian-Eulerian Formulation. *Procedia Engineering* **175**, 273–278.

Kouretzis, G.P., Sheng, D., and Wang, D. 2014. Numerical simulation of cone penetration testing using a new critical state constitutive model for sand. *Computers and Geotechnics* **56**, 50–60.

Liyanapathirana, D.S. 2009. Arbitrary Lagrangian Eulerian based finite element analysis of cone penetration in soft clay. *Computers and Geotechnics* **36**, 851–860.

Mozaffari, M., and Ghafghazi, M. 2017. Implementation of NorSand in Abaqus. *GeoOttawa 2017* (Eds: Fall M. & Simms P.). Ottawa, Ontario, Canada.

Mozaffari, M., and Ghafghazi, M. 2019. A Numerical Study of the Effects of Contact Friction on CPT Results. *GeoSt.John's 2019* (Eds: Parsons S. & Dhar A.). St John's, Newfoundland and Labrador, Canada.

Mozaffari, M., and Ghafghazi, M. 2023. Material-Specific Interpretation of the State Parameter from Drained Cone Penetration Tests. *Canadian Geotechnical Journal*, Accepted.

Potyondy, J.G. 1961. Skin Friction between Various Soils and Construction Materials. *Géotechnique*, **11,** 339–353.

Price, A.B., Boulanger, R.W., and DeJong, J.T. 2019. Centrifuge Modeling of Variable-Rate Cone Penetration in Low-Plasticity Silts. *Journal of Geotechnical and Geoenvironmental Engineering* **145**, 4019098.

Sheng, D., Cui, L., and Ansari, Y. 2013. Interpretation of cone factor in undrained soils via full-penetration finite-element analysis. *International Journal of Geomechanics* **13**, 745–753.

Sheng, D., Kelly, R., Pineda, J., and Bates, L. 2014. Numerical study of rate effects in cone penetration test. *Proceedings, 3rd International Symposium on Cone Penetration Testing* (Eds: Robertson P.K. & Cabal K.L.), 419–428. Las Vegas, Nevada, USA.

Shuttle, D., and Jefferies, M. 2016. Determining silt state from CPTu. *Geotechnical Research*, **3**, 90–118.

Shuttle, D.A., and Cunning, J. 2007. Liquefaction potential of silts from CPTu. *Canadian Geotechnical Journal* **44**, 1–19.

Simo, J.C., and Taylor, R.L. 1986. A return mapping algorithm for plane stress elastoplasticity. *International Journal for Numerical Methods in Engineering* **22**, 649–670.